This article has been accepted for publication in a future issue of this journal, but has not been fully edited. Content may change prior to final publication. Citation information: DOI 10.1109/TIA.2020.3009311, IEEE Transactions on Industry Applications

Control of Three-Phase Power Electronic Converter with Power Controllers in Stationary Frame

Sebastian Wodyk, Grzegorz Iwanski, *Senior Member, IEEE*

***Abstract*— This paper concentrates on a three-phase power converter control system that uses voltages and currents in a stationary reference frame. The advantages of such a control system include lack of transformation between stationary and rotating reference frames and hence no need for an extra algorithm such as a phase locked loop for the grid voltage phase angle determination, as the power components are the same in every coordinates system. The method proposed in this paper uses PResI controllers for tracking referenced Akagi's instantaneous power components, which contain intentional oscillations of double grid frequency. Thanks to that, the sinusoidal converter current is maintained despite the negative sequence component in grid voltage. Different targets for converter current asymmetry, from corresponding, through symmetrical, to opposite to voltage asymmetry may be achieved, depending on the operation mode and the demanded power. Moreover, the power limitation method allowing limitation of the phase current amplitude even for unbalanced phase currents was applied.**

***Index Terms*— AC-DC power converters, direct power control, power limiters, unbalanced grid**

I. Introduction

GRID-CONNECTED three-phase power converters (Fig. 1) play a significant role in a utility grid. They are used with the aim of an electrical energy quality improvement, as well as bi-directional energy transfer between the line and DC circuits, which can be railway electric traction, electrical energy storage, or DC-link of active rectifiers or inverters utilized in renewable energy conversion systems, etc. Thanks to that, sinusoidal current waveform and control of power flow with a high power factor is possible.

One of the most popular control strategies uses proportional-integral (PI) controllers in order to control components of the current vector, oriented with respect to the grid voltage vector (Voltage Oriented Control - VOC) in a dq synchronous reference frame [2][3]. Another popular method is direct power control (DPC), which uses hysteresis controllers of instantaneous power p, q components [4]. Both methods require determination of the grid voltage phase angle. Due to that, further improvements, like phase-locked-loop (PLL) [5], virtual-flux-orientation of the synchronous reference frame

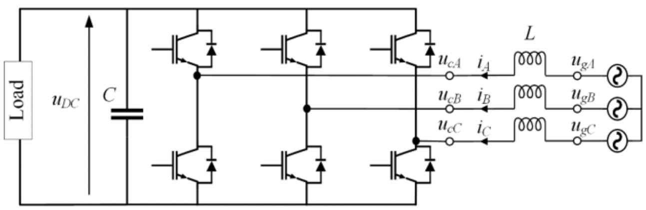

Fig. 1. Scheme of a grid-connected three-phase power converter.

(VFOC) [6], or virtual flux-based estimation of instantaneous power (VF-DPC) [7] were proposed. In order to obtain constant switching frequency for direct power control methods, space-vector modulation instead of a switching table was proposed (DPC-SVM) [8]. Application of PLL, as well as virtual-flux in control systems allowed to reduce the content of converter current high harmonics caused by grid voltage harmonics. However, such methods were still sensitive to grid voltage asymmetry. The negative sequence component of grid voltage introduces phase angle oscillation, as the voltage hodograph is no longer circular, but elliptical. Due to that, transformation to synchronous reference is much more difficult.

In order to avoid coordinate transformation, the stationary frame control system may be applied, where the zero steady state current error is provided by proportional-resonant (PR) controllers [9]-[14]. Thanks to lack of the synchronous reference frame transformation there is no need for grid voltage phase angle determination, thus synchronization issues are eliminated, which is an advantage in the case of grid voltage imbalance [15]-[21]. Nevertheless, such a control system demands accurate sinusoidal reference generators, which has recently become an important research issue. In [15], the authors proposed a current reference determination method based on symmetrical sequence components extraction of grid voltage and the converter control signal, as well as average values of instantaneous power components. The main assumption was minimization of DC voltage ripples, which naturally leads to current asymmetry opposite to voltage asymmetry, because the *p* component of instantaneous power is not oscillating in such a case. For the presented rectifier operation mode, the proposed method is unfavorable to the grid, because the phase with the lowest rms voltage values is loaded the most. Similar results were achieved by the authors of [16], but without symmetrical sequence extraction. Manipulation of

.

0093-9994 (c) 2020 IEEE. Personal use is permitted, but republication/redistribution requires IEEE permission. See http://www.ieee.org/publications_standards/publications/rights/index.html for more information.
Authorized licensed use limited to: POLITECHNIKI WARSZAWSKIEJ. Downloaded on July 15,2020 at 23:38:25 UTC from IEEE Xplore. Restrictions apply.

This article has been accepted for publication in a future issue of this journal, but has not been fully edited. Content may change prior to final publication. Citation information: DOI 10.1109/TIA.2020.3009311, IEEE Transactions on Industry Applications

the current asymmetry factor was proposed in [17]. The authors introduced adaptable parameters in the reference generator which was based on grid voltage symmetrical sequence components decomposition. Unfortunately, experimental results show strongly distorted current. Papers [15]-[17] do not present current limitation. For the asymmetrical current limitation it is not a trivial issue, because its vector representation does not translate into three phase representation as easily as in the case of symmetrical current. Therefore, for the sake of proper limitation, some additional three-phase structures were proposed [18]-[20].

Another approach to the control of grid connected converters operating under asymmetrical voltage sags is modification of classic structures with PI current controllers. Then, regulation is done in two synchronous reference frames, where one is oriented along the grid voltage positive sequence, and the second is oriented along the negative sequence [21][22] vector component. Additionally, notch filters of negative sequence *dq* current are often utilized in such systems [22], which narrows the bandwidth of the current control. A symmetrical current target is easy to realize by setting the reference negative sequence current to zero, although it is not fully beneficial to the grid.

Some modifications of DPC-SVM methods were proposed in the literature, like low-pass filtering of the virtual flux magnitude and PLL to synchronization of the virtual flux phase angle [23]. As the instantaneous power components are independent on the reference frame orientation or rotation, the direct power control methods can be realized without PLL structures, whereas synchronization of the converter current to the grid voltage results in the control algorithm itself. It has recently become popular research issue [1][24][25]. Although control systems presented in [1] and [24] are similar, it can be noticed that in [1] impact of grid voltage harmonics on a current shape is lower. Both papers do not consider unbalanced voltage dips. Another method was proposed in [25], which is power reference compensation based on current and voltage symmetrical sequence decomposition and current third harmonic extraction, as well as proportional-resonant-integral controllers (PResI) to track the reference. The authors did not consider grid voltage harmonics; moreover, results presented in the paper do not show step change of the average power components, thus dynamics is difficult in the evaluation. The DPC strategy can be realized without symmetrical sequence decomposition, but with a grid voltage vector quadrature component (voltage vector delayed by $\pi/2$), as proposed in [26] and [27] in deadbeat based control systems, which requires precise determination of grid filter parameters.

An appropriate asymmetry of current obtained by the control system is beneficial to the grid, because in the rectifier mode, the phase with the lowest voltage rms values is loaded the least, and in the inverter mode it is supported the most. However, the maximal converter power cannot be delivered, because some of the legs operate below their maximal allowable current. A solution of this issue is current balancing at the time when demanded power is above the value resulting from asymmetrical current limitation. In [28], the authors presented a method allowing intermediate current asymmetry between opposite to grid voltage asymmetry and symmetrical current. Such an approach is beneficial to the grid only in the inverter operation mode. Moreover, reactive power support was not analyzed.

This paper proposes a novel direct power control system, able to operate under asymmetrical grid voltage. Main features of the system are:

1) determination of the instantaneous power components oscillations, causing desired current asymmetry,

2) limitation of the reference instantaneous power components average values, which results in limitation of the current, in such a way that the greatest amplitude between three-phase currents does not exceed assumed maximal values,

3) current balancing method, allowing apparent power maximization, when limit for asymmetrical current is achieved.

Intermediate current asymmetry is achieved immediately depending on the demanded apparent power. The control system does not contain *dq* transformation, and thus there is no need for special structures of reference frame synchronization, so no grid voltage phase angle estimation like PLL is needed. Converter control signals are calculated on the basis of stationary frame grid voltage and outputs of PResI instantaneous power controllers, taking into account decoupling terms in the control signals. In order to provide the desired current asymmetry, keeping sinusoidal waveform, appropriate power components oscillations are determined and added to the reference. This paper presents theoretical considerations, as well as their simulation and experimental verification.

II. Stationary Frame Control System

A lack of transformation between rotating and stationary reference frames eliminates phase angle determination issues associated with grid voltage asymmetry. Thus, a control system with power controllers in a stationary reference frame has been proposed. Therefore, it is proposed to use instantaneous power *pq*, described by (1) and (2), as control variables.

$$p = \frac{3}{2}\left(u_{g\alpha} i_{L\alpha} + u_{g\beta} i_{L\beta}\right) \tag{1}$$

$$q = \frac{3}{2}\left(u_{g\beta} i_{L\alpha} - u_{g\alpha} i_{L\beta}\right) \tag{2}$$

where $i_{L\alpha}$, $i_{L\beta}$ – converter current vector components, $u_{g\alpha}$, $u_{g\beta}$ – grid voltage vector components. The current vector may be presented as follows:

$$i_{L\alpha} = \frac{2}{3}\left(\frac{u_{g\alpha}}{u_{g\alpha}^2 + u_{g\beta}^2} p + \frac{u_{g\beta}}{u_{g\alpha}^2 + u_{g\beta}^2} q\right) \tag{3}$$

$$i_{L\beta} = \frac{2}{3}\left(\frac{u_{g\beta}}{u_{g\alpha}^2 + u_{g\beta}^2} p - \frac{u_{g\alpha}}{u_{g\alpha}^2 + u_{g\beta}^2} q\right) \tag{4}$$

Voltage equations of a three-phase grid-connected power converter can be described by instantaneous power components, instead of a current:

$$u_{c\alpha} = -\frac{2}{3} R \left(\frac{p u_{g\alpha} + q u_{g\beta}}{u_{g\alpha}^2 + u_{g\beta}^2}\right) - \frac{2}{3} L \frac{d}{dt}\left(\frac{p u_{g\alpha} + q u_{g\beta}}{u_{g\alpha}^2 + u_{g\beta}^2}\right) + u_{g\alpha} \tag{5}$$

0093-9994 (c) 2020 IEEE. Personal use is permitted, but republication/redistribution requires IEEE permission. See http://www.ieee.org/publications_standards/publications/rights/index.html for more information.
Authorized licensed use limited to: POLITECHNIKI WARSZAWSKIEJ. Downloaded on July 15,2020 at 23:38:25 UTC from IEEE Xplore. Restrictions apply.

This article has been accepted for publication in a future issue of this journal, but has not been fully edited. Content may change prior to final publication. Citation information: DOI 10.1109/TIA.2020.3009311, IEEE Transactions on Industry Applications

$$u_{c\beta} = -\frac{2}{3}R\left(\frac{pu_{g\beta}-qu_{g\alpha}}{u_{g\alpha}^2+u_{g\beta}^2}\right)-\frac{2}{3}L\frac{d}{dt}\left(\frac{pu_{g\beta}-qu_{g\alpha}}{u_{g\alpha}^2+u_{g\beta}^2}\right)+u_{g\beta} \tag{6}$$

where u_c - converter voltage vector, u_g - grid voltage vector, R – inductor resistance, L – filter inductance, p, q – instantaneous power components. Derivatives of the current vector components can be described as:

$$\frac{d}{dt}i_{L\alpha} = \frac{2}{3}\left(\frac{dp}{dt}\frac{u_{g\alpha}}{u_{g\alpha}^2+u_{g\beta}^2}+\frac{dq}{dt}\frac{u_{g\beta}}{u_{g\alpha}^2+u_{g\beta}^2}+r_\alpha\right) \tag{7}$$

$$\frac{d}{dt}i_{L\beta} = \frac{2}{3}\left(\frac{dp}{dt}\frac{u_{g\beta}}{u_{g\alpha}^2+u_{g\beta}^2}-\frac{dq}{dt}\frac{u_{g\alpha}}{u_{g\alpha}^2+u_{g\beta}^2}+r_\beta\right) \tag{8}$$

where:

$$r_\alpha = \frac{du_{g\alpha}}{dt}\frac{p\left(u_{g\beta}^2-u_{g\alpha}^2\right)-2qu_{g\alpha}u_{g\beta}}{\left(u_{g\alpha}^2+u_{g\beta}^2\right)^2}+\frac{du_{g\beta}}{dt}\frac{q\left(u_{g\alpha}^2-u_{g\beta}^2\right)-2pu_{g\alpha}u_{g\beta}}{\left(u_{g\alpha}^2+u_{g\beta}^2\right)^2} \tag{9}$$

$$r_\beta = \frac{du_{g\alpha}}{dt}\frac{q\left(u_{g\alpha}^2-u_{g\beta}^2\right)-2pu_{g\alpha}u_{g\beta}}{\left(u_{g\alpha}^2+u_{g\beta}^2\right)^2}-\frac{du_{g\beta}}{dt}\frac{p\left(u_{g\beta}^2-u_{g\alpha}^2\right)-2qu_{g\alpha}u_{g\beta}}{\left(u_{g\alpha}^2+u_{g\beta}^2\right)^2} \tag{10}$$

It can be noticed that the overall current derivative, and in consequence, voltage drop on inductor reactance can be fundamentally divided into two parts. The first one relates to instantaneous power components (r_α, r_β), and the second one relates to their derivatives. Considering non-distorted, symmetrical grid voltage and current, part of an inductor voltage drop resulting from power components derivatives will be equal to zero for the steady state, whereas r_α, r_β will stand for the coupling between p and q [1]. However, while a negative sequence component of grid voltage occurs, in order to maintain sinusoidal current waveforms, instantaneous power components need to contain certain oscillations of double grid frequency. Therefore, derivatives of power components are no longer equal to zero for steady states, and part of an inductor voltage drop related to them is not equal to zero as well. Moreover, r_α and r_β do not represent only coupling between power components, but also contain some part resulting from themselves. Both mentioned parts of the inductor voltage drop do not take sinusoidal waveform, but their sum is sinusoidal, as can be seen in Fig. 2A. Equations (5) and (6) can be written in the matrix form, as follows:

$$\begin{bmatrix}u_{c\alpha}\\u_{c\beta}\end{bmatrix} = \frac{-1}{u_{g\alpha}^2+u_{g\beta}^2}\begin{bmatrix}u_{g\alpha} & u_{g\beta}\\u_{g\beta} & -u_{g\alpha}\end{bmatrix}\frac{2}{3}\begin{bmatrix}Rp+L\frac{\mathrm{d}p}{\mathrm{d}t}+Lr_p\\Rq+L\frac{\mathrm{d}q}{\mathrm{d}t}+Lr_q\end{bmatrix}+\begin{bmatrix}u_{g\alpha}\\u_{g\beta}\end{bmatrix} \tag{11}$$

where

$$r_p = -p\frac{\frac{du_{g\alpha}}{dt}u_{g\alpha}+\frac{du_{g\beta}}{dt}u_{g\beta}}{u_{g\alpha}^2+u_{g\beta}^2}-q\frac{\frac{du_{g\alpha}}{dt}u_{g\beta}-\frac{du_{g\beta}}{dt}u_{g\alpha}}{u_{g\alpha}^2+u_{g\beta}^2} \tag{12}$$

$$r_q = -p\frac{\frac{du_{g\beta}}{dt}u_{g\alpha}-\frac{du_{g\alpha}}{dt}u_{g\beta}}{u_{g\alpha}^2+u_{g\beta}^2}-q\frac{\frac{du_{g\alpha}}{dt}u_{g\alpha}+\frac{du_{g\beta}}{dt}u_{g\beta}}{u_{g\alpha}^2+u_{g\beta}^2} \tag{13}$$

Inductor voltage drop transformed to the power components related reference frame is described directly by derivatives of p and q, as well as r_p and r_q which include coupling between power components. Both parts consist of dc values combined with double grid frequency oscillations, which is illustrated in Fig. 2b. Calculation of r_p and r_q, in general, is not trivial because it requires differentiation of the measured grid voltage, which results in amplification of measuring noise and other disturbances. However, considering only fundamental harmonic it can be assumed that:

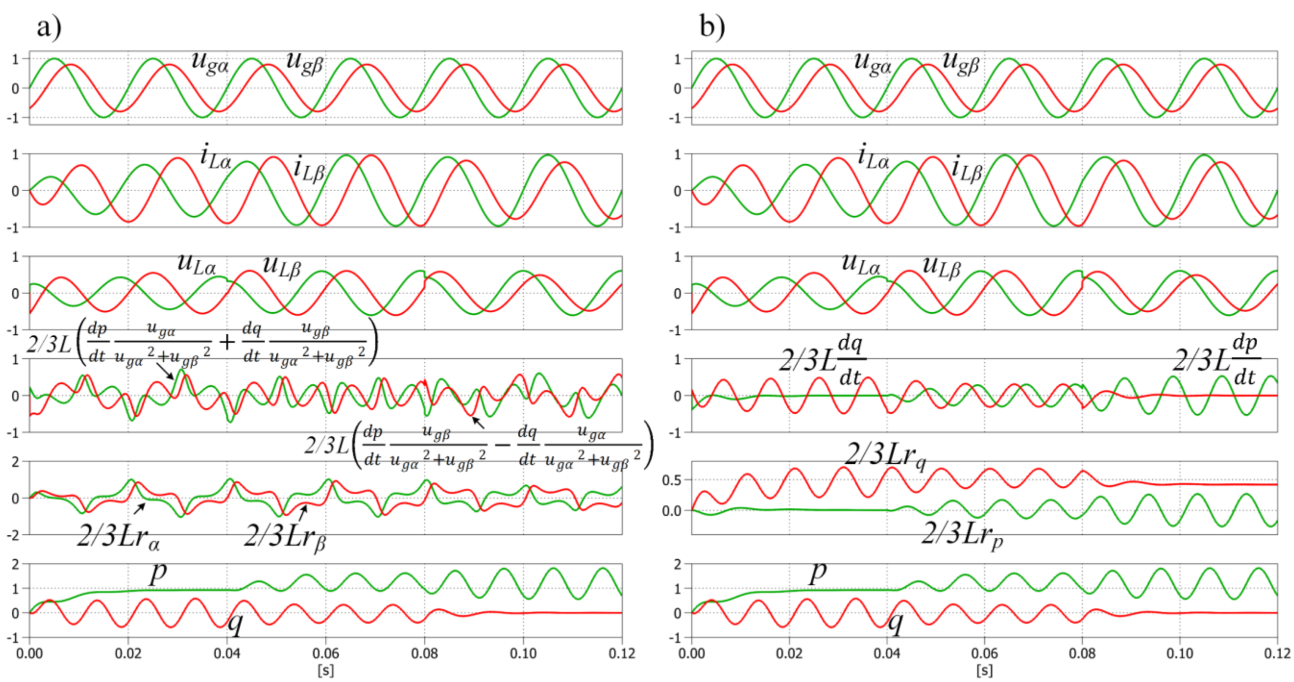

Fig. 2. Example of voltage drop on 2 mH ideal inductor during change of instantaneous power components, for different current targets, u_g – line voltage (p. u.), i_L – inductor current (p. u.), u_L – inductor voltage drop (p. u.), p, q- instantaneous power components (p. u.). a) representation in $\alpha\beta$ frame, b) values related to p and q.

0093-9994 (c) 2020 IEEE. Personal use is permitted, but republication/redistribution requires IEEE permission. See http://www.ieee.org/publications_standards/publications/rights/index.html for more information.
Authorized licensed use limited to: POLITECHNIKI WARSZAWSKIEJ. Downloaded on July 15,2020 at 23:38:25 UTC from IEEE Xplore. Restrictions apply.

This article has been accepted for publication in a future issue of this journal, but has not been fully edited. Content may change prior to final publication. Citation information: DOI 10.1109/TIA.2020.3009311, IEEE Transactions on Industry Applications

$$\frac{d}{dt}u_{g\alpha} = -\omega u_{g\alpha}^{q} \qquad (14)$$

$$\frac{d}{dt}u_{g\beta} = -\omega u_{g\beta}^{q} \qquad (15)$$

where ω – grid voltage pulsation, $u_{g\alpha}^{q}$, $u_{g\beta}^{q}$ – grid voltage vector quadrature components, which may be obtained by second order generalized integrator SOGI filtration [29]. Additionally, harmonic filtration of grid voltage direct components signals ($u_{g\alpha}^{d}$, $u_{g\beta}^{d}$) is achieved, which is beneficial for the control system, because voltage harmonics produce unwanted oscillations in power components signals, which leads to converter current distortions. Using filtered signals, it can be written that:

$$r_p = \omega p \frac{u_{g\alpha}^{d}u_{g\alpha}^{q}+u_{g\beta}^{d}u_{g\beta}^{q}}{u_{g\alpha}^{d\,2}+u_{g\beta}^{d\,2}} - \omega q \frac{u_{g\alpha}^{d}u_{g\beta}^{q}-u_{g\beta}^{d}u_{g\alpha}^{q}}{u_{g\alpha}^{d\,2}+u_{g\beta}^{d\,2}} \qquad (16)$$

$$r_q = \omega p \frac{u_{g\alpha}^{d}u_{g\beta}^{q}-u_{g\beta}^{d}u_{g\alpha}^{q}}{u_{g\alpha}^{d\,2}+u_{g\beta}^{d\,2}} + \omega q \frac{u_{g\alpha}^{d}u_{g\alpha}^{q}+u_{g\beta}^{d}u_{g\beta}^{q}}{u_{g\alpha}^{d\,2}+u_{g\beta}^{d\,2}} \qquad (17)$$

A. Calculation of the reference instantaneous power components oscillations

In order to maintain sinusoidal converter current waveform, adequate p and q power components oscillations need to be referenced. Two general targets of current asymmetry may be achieved, which are current asymmetry opposite to voltage asymmetry (target I), and current asymmetry corresponding to voltage asymmetry (target II), whereas intermediate states are a mix of these two targets. Target I is beneficial to the grid in the inverter operation mode and target II in the rectifier operation mode, while intermediate states allow an increase of the available converter power. Grid voltage vector components, considering only fundamental harmonic, can be described as follows:

$$u_{\alpha} = U_{\alpha m}\sin(\omega t + \alpha_u) \qquad (18)$$

$$u_{\beta} = -U_{\beta m}\cos(\omega t + \beta_u) \qquad (19)$$

where $U_{\alpha m}$, $U_{\beta m}$ – amplitudes of grid voltage vector components, α_u, β_u – phase shifts between corresponding vector components and its positive sequence component, ω – fundamental harmonic pulsation. Accordingly, current vector fundamental harmonic can be described as:

$$i_{\alpha} = I_{\alpha m}\sin(\omega t + \varphi + \alpha_i) \qquad (20)$$

$$i_{\beta} = -I_{\beta m}\cos(\omega t + \varphi + \beta_i) \qquad (21)$$

where φ - phase shift between positive sequence components of voltage and current vectors. Depending on the desired target, α_i, β_i correspond to the voltage phase shifts directly or crosswise. Similarly, $I_{\alpha m}$, $I_{\beta m}$ are proportional to the voltage amplitudes directly or crosswise. Then, basing on equations (1) and (2), power components oscillations can be described by (22) and (23) for target I and (24) and (25) for target II.

$$p = 3I_{m_{avg}}\frac{U_{\alpha m}U_{\beta m}}{U_{\alpha m}+U_{\beta m}}\cos(\alpha_u - \beta_u)\cos(\varphi) \qquad (22)$$

$$q = -\frac{3}{2}I_{m_{avg}}\frac{U_{\alpha m}^2+U_{\beta m}^2}{U_{\alpha m}+U_{\beta m}}\sin(\varphi) + \frac{3}{2}\frac{I_{m_{avg}}}{U_{\alpha m}+U_{\beta m}}[\cos(\varphi)\,(U_{\alpha m}^2\sin(2\omega t + 2\alpha_u) - U_{\beta m}^2\sin(2\omega t + 2\beta_u)) + \sin(\varphi)(U_{\alpha m}^2\cos(2\omega t + 2\alpha_u) - U_{\beta m}^2\cos(2\omega t + 2\beta_u))] \qquad (23)$$

$$p = \frac{3}{2}I_{m_{avg}}\frac{U_{\alpha m}^2+U_{\beta m}^2}{U_{\alpha m}+U_{\beta m}}\cos(\varphi) + \frac{3}{2}\frac{I_{m_{avg}}}{U_{\alpha m}+U_{\beta m}}[\cos(\varphi)\,(U_{\beta m}^2\cos(2\omega t + 2\beta_u) - U_{\alpha m}^2\cos(2\omega t + 2\alpha_u)) - \sin(\varphi)(U_{\beta m}^2\sin(2\omega t + 2\beta_u) - U_{\alpha m}^2\sin(2\omega t + 2\alpha_u))] \qquad (24)$$

$$q = -3I_{m_{avg}}\frac{U_{\alpha m}U_{\beta m}}{U_{\alpha m}+U_{\beta m}}\cos(\alpha_u - \beta_u)\sin(\varphi) \qquad (25)$$

where $I_{m_{avg}} = \frac{I_{\alpha m}+I_{\beta m}}{2}$. Then oscillating parts of power components $\tilde{p}$, $\tilde{q}$, can be calculated with the use of grid voltage direct and quadrature components and dc parts of power components $\bar{p}$, $\bar{q}$, as follows, for target I:

$$\tilde{p} = 0 \qquad (26)$$

$$\tilde{q} = \bar{p}\frac{u_{g\alpha}^{d}u_{g\alpha}^{q}+u_{g\beta}^{d}u_{g\beta}^{q}}{u_{g\alpha}^{d}u_{g\beta}^{q}-u_{g\beta}^{d}u_{g\alpha}^{q}} - \bar{q}\frac{u_{g\alpha}^{q\,2}+u_{g\beta}^{q\,2}-u_{g\alpha}^{d\,2}-u_{g\beta}^{d\,2}}{u_{g\alpha}^{q\,2}+u_{g\beta}^{q\,2}+u_{g\alpha}^{d\,2}+u_{g\beta}^{d\,2}} \qquad (27)$$

and for target II:

$$\tilde{p} = -\bar{p}\frac{u_{g\alpha}^{q\,2}+u_{g\beta}^{q\,2}-u_{g\alpha}^{d\,2}-u_{g\beta}^{d\,2}}{u_{g\alpha}^{q\,2}+u_{g\beta}^{q\,2}+u_{g\alpha}^{d\,2}+u_{g\beta}^{d\,2}} - \bar{q}\frac{u_{g\alpha}^{d}u_{g\alpha}^{q}+u_{g\beta}^{d}u_{g\beta}^{q}}{u_{g\alpha}^{d}u_{g\beta}^{q}-u_{g\beta}^{d}u_{g\alpha}^{q}} \qquad (28)$$

$$\tilde{q} = 0 \qquad (29)$$

However, for intermediate current asymmetry both power components oscillate (see Fig. 2), so an additional factor ξ, which decides about the share of the oscillating part in each power component, is proposed. Then, oscillating parts can be expressed as:

$$\tilde{p} = \xi\left(-\bar{p}\frac{u_{g\alpha}^{q\,2}+u_{g\beta}^{q\,2}-u_{g\alpha}^{d\,2}-u_{g\beta}^{d\,2}}{u_{g\alpha}^{q\,2}+u_{g\beta}^{q\,2}+u_{g\alpha}^{d\,2}+u_{g\beta}^{d\,2}} - \bar{q}\frac{u_{g\alpha}^{d}u_{g\alpha}^{q}+u_{g\beta}^{d}u_{g\beta}^{q}}{u_{g\alpha}^{d}u_{g\beta}^{q}-u_{g\beta}^{d}u_{g\alpha}^{q}}\right) \qquad (30)$$

$$\tilde{q} = (1-\xi)\left(\bar{p}\frac{u_{g\alpha}^{d}u_{g\alpha}^{q}+u_{g\beta}^{d}u_{g\beta}^{q}}{u_{g\alpha}^{d}u_{g\beta}^{q}-u_{g\beta}^{d}u_{g\alpha}^{q}} - \bar{q}\frac{u_{g\alpha}^{q\,2}+u_{g\beta}^{q\,2}-u_{g\alpha}^{d\,2}-u_{g\beta}^{d\,2}}{u_{g\alpha}^{q\,2}+u_{g\beta}^{q\,2}+u_{g\alpha}^{d\,2}+u_{g\beta}^{d\,2}}\right) \qquad (31)$$

Seeing that (30) and (31) describe reference values, they are calculated with the reference $\bar{p}$ and $\bar{q}$. Determination of the factor ξ value depends on the power limitation as well as converter operation mode.

B. Power components limitation with accordance to the maximal amplitude of the phase current

Limitation of the power components should ensure that current in any phase will not exceed the maximum allowable RMS value. Otherwise, a converter may break down due to overheating of the semiconductor devices and inductor saturation may occur if they are both designed in a low margin of over-sizing. Considering sinusoidal converter current waveform, maximal power is achieved for symmetrical current. On the other hand, such a situation is not beneficial to the grid during asymmetrical sags and therefore intermediate current

0093-9994 (c) 2020 IEEE. Personal use is permitted, but republication/redistribution requires IEEE permission. See http://www.ieee.org/publications_standards/publications/rights/index.html for more information.
Authorized licensed use limited to: POLITECHNIKI WARSZAWSKIEJ. Downloaded on July 15,2020 at 23:38:25 UTC from IEEE Xplore. Restrictions apply.

This article has been accepted for publication in a future issue of this journal, but has not been fully edited. Content may change prior to final publication. Citation information: DOI 10.1109/TIA.2020.3009311, IEEE Transactions on Industry Applications

asymmetry (between target I and target II) should be maintained only if demanded power is greater than limits for a given target. Taking into account dc parts of the equations (22) and (24), maximal dc parts of the power components may be calculated in a similar way like reference oscillating parts. Equations (32) and (33) describe the maximal p component, assuming that $\cos(\varphi) = 1$, for both asymmetrical current targets ($|\bar{p}_I|$, $|\bar{p}_{II}|$).

$$|\bar{p}_I| = \left|3I_{max}\frac{u_{g\beta}^d u_{g\alpha}^q - u_{g\alpha}^d u_{g\beta}^q}{2\max\{U_I\}}\right| \quad (32)$$

$$|\bar{p}_{II}| = \left|\frac{3}{2}I_{max}\frac{u_{g\alpha}^{q\,2}+u_{g\beta}^{q\,2}+u_{g\alpha}^{d\,2}+u_{g\beta}^{d\,2}}{2\max\{U_{II}\}}\right| \quad (33)$$

where I_{max} – maximal rated amplitude of the three-phase current, $U_{II} = [U_{AII}\ U_{BII}\ U_{CII}]$ amplitudes of the three-phase grid voltage, $U_I = [U_{AI}\ U_{BI}\ U_{CI}]$ - amplitudes of the theoretical three-phase voltage of asymmetry opposite to grid voltage.

Assuming that the current is approximately symmetrical for $\xi = 0.5$ the maximal available dc part of the p component may be expressed as follows:

$$|\bar{p}_{max}| = \left|\frac{3}{2}I_{max}\left(\frac{\left(u_{g\alpha}^d - u_{g\beta}^q\right)^2 + \left(u_{g\beta}^d + u_{g\alpha}^q\right)^2}{U_p}\right)\right| \quad (34)$$

where U_p – amplitude of a grid voltage positive sequence component.

$$U_{AI} = \sqrt{u_{g\beta}^{d\,2}+u_{g\beta}^{q\,2}} \quad (35)$$

$$U_{BI} = \frac{1}{2}\sqrt{\left(u_{g\beta}^d + \sqrt{3}u_{g\alpha}^d\right)^2 + \left(u_{g\beta}^q + \sqrt{3}u_{g\alpha}^q\right)^2} \quad (36)$$

$$U_{CI} = \frac{1}{2}\sqrt{\left(u_{g\beta}^d - \sqrt{3}u_{g\alpha}^d\right)^2 + \left(u_{g\beta}^q - \sqrt{3}u_{g\alpha}^q\right)^2} \quad (37)$$

$$U_{AII} = \sqrt{u_{g\alpha}^{d\,2}+u_{g\alpha}^{q\,2}} \quad (38)$$

$$U_{BII} = \frac{1}{2}\sqrt{\left(u_{g\alpha}^d + \sqrt{3}u_{g\beta}^d\right)^2 + \left(u_{g\alpha}^q + \sqrt{3}u_{g\beta}^q\right)^2} \quad (39)$$

$$U_{CII} = \frac{1}{2}\sqrt{\left(u_{g\alpha}^d - \sqrt{3}u_{g\beta}^d\right)^2 + \left(u_{g\alpha}^q - \sqrt{3}u_{g\beta}^q\right)^2} \quad (40)$$

$$U_p = \frac{1}{2}\sqrt{\left(u_{g\alpha}^d - u_{g\beta}^q\right)^2 + \left(u_{g\alpha}^q + u_{g\beta}^d\right)^2} \quad (41)$$

Basing on (23) and (25) limitation of the q component dc part may be calculated in the same way as for the p component, as follows:

$$|\bar{q}_{max}| = \left|\frac{3}{2}I_{max}\left(\frac{\left(u_{g\alpha}^d - u_{g\beta}^q\right)^2 + \left(u_{g\beta}^d + u_{g\alpha}^q\right)^2}{U_p}\right)\right| \sin(\varphi)_{max} \quad (42)$$

where

$$\sin(\varphi)_{max} = \sqrt{1 - \left(\frac{\bar{p}^*}{|\bar{p}_{max}|}\right)^2} \quad (43)$$

$$|\bar{q}_{max}| = \sqrt{|\bar{p}_{max}|^2 - \bar{p}^{*\,2}} \quad (44)$$

Limitation of the q component of the instantaneous dc part power depends on the reference $\bar{p}^*$, in order to keep the priority of active power.

C. Determination of the ξ factor value

Introduction of the ξ factor allows smooth change of the current asymmetry. It is particularly important in case of exceeding limits arising from asymmetrical current limitation. Considering target selection dependent on the converter operation mode, it can be assumed that $\xi \le 0.5$ for $\bar{p}^* < 0$ (inverter mode) and $\xi \ge 0.5$ for $\bar{p}^* > 0$ (rectifier mode). As $\xi = 0.5$ stands for the maximal power point, it can occur for both rectifier and inverter mode. The value of ξ depends also on the reference average apparent power expressed as:

$$s^* = \sqrt{\bar{p}^{*\,2} + \bar{q}^{*\,2}} \quad (45)$$

Then, factor ξ may be presented as a linear function of s^*, as follows:

$$\xi(s^*) = \begin{cases} \frac{|\bar{p}_I| - s^*}{2(|\bar{p}_I| - |\bar{p}_{max}|)} & \text{for } \bar{p}^* < 0 \\ \frac{s^* - |\bar{p}_{max}|}{2(|\bar{p}_{II}| - |\bar{p}_{max}|)} + 0.5 & \text{for } \bar{p}^* > 0 \end{cases} \quad (46)$$

Additional constraints need to be implemented, like $0 \le \xi \le 0.5$ for $\bar{p}^* < 0$, and $0.5 \ge \xi \ge 1$ for $\bar{p}^* > 0$. Fig. 3 presents the graph of the function.

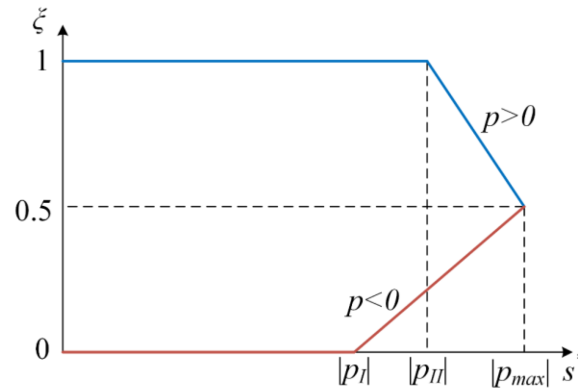

Fig. 3. Graph representing function $\xi(s^*)$.

D. Overall control system with DC-link voltage regulation

The final control system with referenced power oscillations and limitation terms is shown in Fig. 4. In order to control the DC-link voltage, a PI controller is used, but it should be noticed that for target II (oscillating p component), DC-link voltage also oscillates, with double ω grid pulsation. Moreover, grid voltage high harmonics produce additional distortions. Thus, band-stop filtration of 2ω oscillations, and possibly low-pass filtration, in case of a high amount of harmonics in the grid voltage, should be implemented [19]. Anti-windup of the DC-link voltage controller realizes referenced average p power component limitation.

As the q component reference is set arbitrarily, it is limited directly. Limits are calculated basing on the assumed maximal current amplitude I_{max}, as well as filtrated grid voltage direct and quadrature vectors components, provided by SOGI. Then, limited signals of referenced instantaneous power components, are used to calculate adequate referenced oscillations, also

0093-9994 (c) 2020 IEEE. Personal use is permitted, but republication/redistribution requires IEEE permission. See http://www.ieee.org/publications_standards/publications/rights/index.html for more information.
Authorized licensed use limited to: POLITECHNIKI WARSZAWSKIEJ. Downloaded on July 15,2020 at 23:38:25 UTC from IEEE Xplore. Restrictions apply.

This article has been accepted for publication in a future issue of this journal, but has not been fully edited. Content may change prior to final publication. Citation information: DOI 10.1109/TIA.2020.3009311, IEEE Transactions on Industry Applications

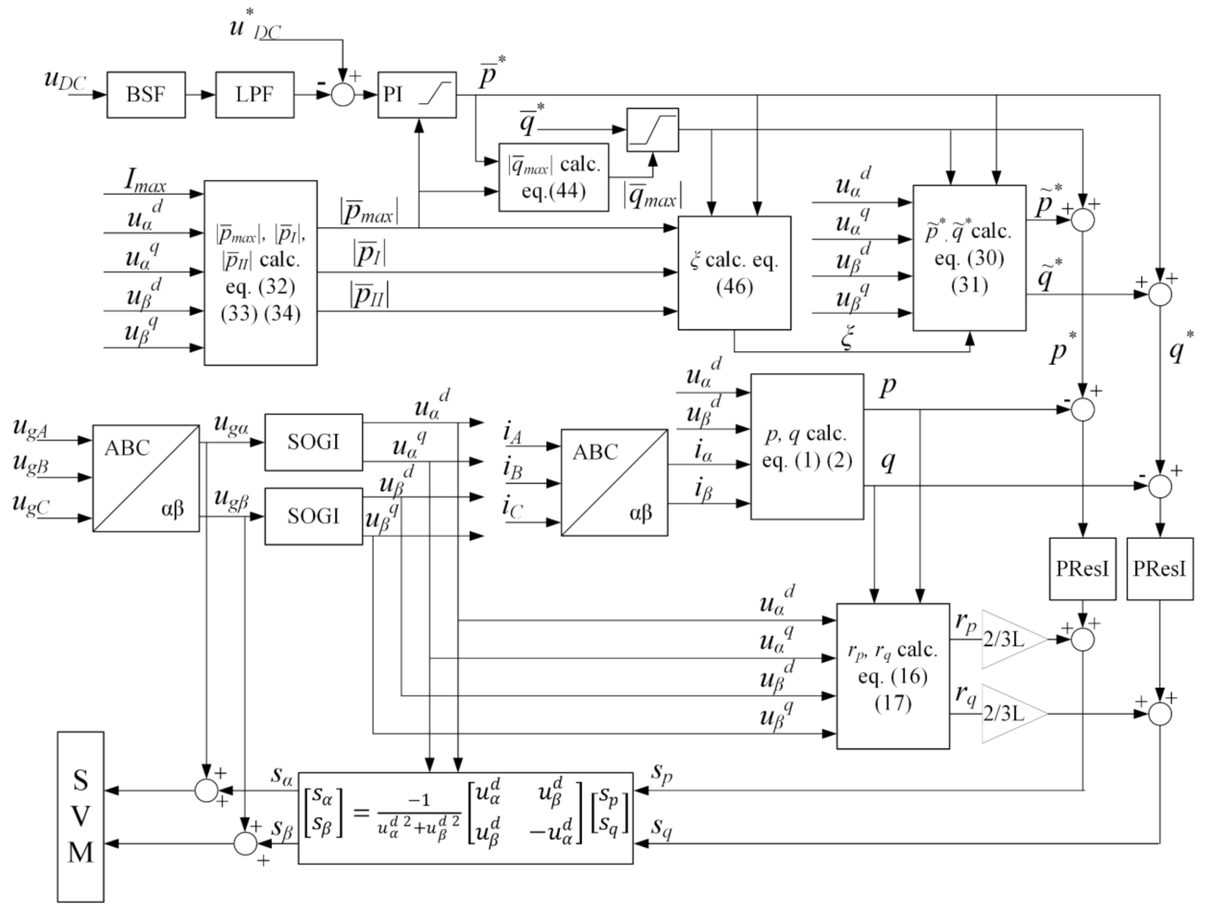

Fig. 4. Block scheme of the proposed control system.

using voltage vectors, created from SOGI outputs.

Instantaneous power components p, q are calculated using filtered grid voltage. This operation is aimed to reduce of unwanted power oscillations due to occurrence of grid voltage harmonics. Thus, instantaneous power components p, q contains only dc values and 2ω oscillations due to voltage and current asymmetry, and influence of harmonics is negligible. Error signals of p and q goes to PResI controllers, which outputs are summed with r_{pq} feedforward multiplied by 2/3 L, and this sum is represented by s_{pq} in Fig. 4. Further, $s_{\alpha\beta}$ signals are calculated using filtered grid voltage, as they are expected to represent voltage drop on a grid filter, which should contain only fundamental harmonic. This expectation is related to use of the original grid voltage feedforward. In practice this feedforward is slightly delayed due to sampling, however all inaccuracies should be compensated by controllers. Finally, converter voltage calculated in this way goes to the SVM.

III. Simulation and Experimental Results

Simulation and experimental tests were carried out with a circuit containing two three-phase two-level IGBT power converters connected by the DC-link, one of which was utilized as a variable load/source. Parameters of the laboratory rig are presented in Table I, and they correspond to the simulation parameters. In the experiment, a DSP controller built with TMS320F28335 was used as the control unit.

TABLE I
Parameters of the simulated circuit

Symbol	Quantity	Value
U_{gn}	Nominal grid voltage (L-L rms)	230 V
I_{max}	Maximal current amplitude	10 A
L	Grid filter inductance	2.5 mH
R	Inductor resistance	40 mΩ
L_T	Transformer leakage inductance	2.3 mH
C_{DC}	DC-link capacitance	1 mF
U_{DC}	Reference DC voltage	390 V
f_s	Switching frequency	10 kHz

The main converter was connected to the transformer giving nominally 3x230 V line-to-line rms voltage directly, whereas the second one (load/source converter) was connected by an isolation transformer in order to provide separation between AC circuits. Both experimental and simulation tests were conducted for a 2-phase voltage dip. Moreover, simulated grid voltage contained 6% of 5th harmonic and 5% of 7th harmonic. Parameters of filters applied in the control system are shown in Table II.

Fig. 5 presents the influence of the r_{pq} feedforward during step change of the average p components. Lack of such feedforward results in visible coupling between instantaneous power components. Introduction of r_{pq} allows to reduce this phenomenon and hence improve control dynamics.

0093-9994 (c) 2020 IEEE. Personal use is permitted, but republication/redistribution requires IEEE permission. See http://www.ieee.org/publications_standards/publications/rights/index.html for more information.
Authorized licensed use limited to: POLITECHNIKI WARSZAWSKIEJ. Downloaded on July 15,2020 at 23:38:25 UTC from IEEE Xplore. Restrictions apply.

This article has been accepted for publication in a future issue of this journal, but has not been fully edited. Content may change prior to final publication. Citation information: DOI 10.1109/TIA.2020.3009311, IEEE Transactions on Industry Applications

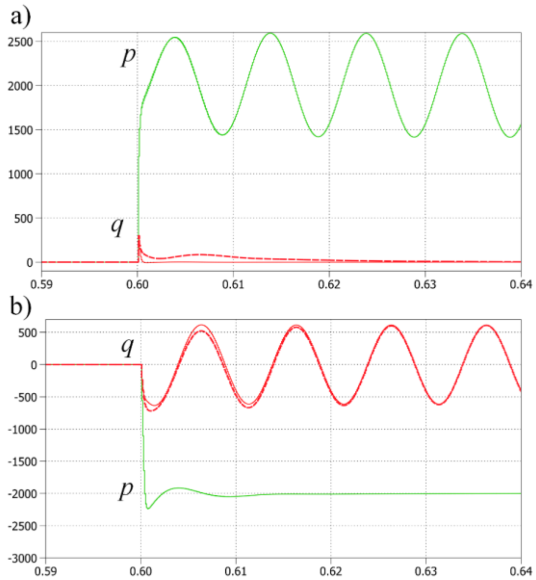

Fig. 5. Results of the simulation presenting influence of the r_{pq} feedforward on step change of the reference average p component. Solid lines represent a system with feedforward, dashed lines represent a system without feedforward.

TABLE II
Parameters of filters used in the simulation and the experiment

Filter	Transfer function	Parameter
BSF	$G(s)=\dfrac{s^2+\omega_0^2}{s^2+\omega_c+\omega_0^2}$	$\omega_0=200\pi$ $\omega_c=20\pi$
LPF	$G(s)=\dfrac{\omega_0^2}{s^2+2\omega_0+\omega_0^2}$	$\omega_0=300\pi$
SOGI	$G_d(s)=\dfrac{k\omega_0 s}{s^2+k\omega_0 s+\omega_0^2}$ $G_q(s)=\dfrac{k{\omega_0}^2}{s^2+k\omega_0 s+\omega_0^2}$	$\omega_0=50\pi$ $k=0.1$

Step change of energy flow in the DC-link is presented in Fig. 6. First, there is an energy surplus and the converter operates in the inverter mode, with current asymmetry opposite to voltage asymmetry. After that, step load of the DC-link occurs and the converter operates in the rectifier mode, current asymmetry corresponds to the voltage asymmetry. Regulation of the DC-link voltage is done with low-pass and band-stop filtration, in order to reduce distortion caused by p component oscillation, as well as grid voltage high harmonics, particularly 5th and 7th harmonic. It deteriorates dynamics of the DC-link voltage control, but does not introduce large enough increase and drop causing disconnection of the converter from the grid. Lack of filtration may cause improper determination of the reference p and q power components oscillations, as well as oscillations of the ξ factor. It can be noticed that step change of energy flow in the DC-link results in temporary current balancing, which enables active power maximization maintaining sinusoidal current waveform to obtain reference DC-bus voltage as fast as possible.

The proposed control system gives the possibility of reactive power support. Step change of the q component for both rectifier and inverter operation mode is presented in Fig. 7. In order to provide a certain mode, active power flow was enforced. Fig. 8 presents a linear change of load/supply power, from low to high saturation level. Both current balancing and limitation can be observed, which is directly associated with power limitation. Current asymmetry changes due to reference power as well as active power sign. In order to achieve intermediate current asymmetry, and finally symmetrical current, oscillation of both power components is introduced. Maximal power is achieved for both rectifier and inverter operation modes. Fig. 9 presents of change of the ξ factor for the same conditions as in Fig. 8. Moreover, grid voltage and current hodographs are presented. Oscillograms start from $\xi = 0.5$. Then, along with reference power change, the ξ factor changes according to equation (46). As can be seen, current hodographs are closed inside a hexagonal area, which represents three-phase current amplitude limitation. The current vector hodograph changes between the elliptical and circular form, depending on the ξ factor value.

Fig. 10-12 present grid voltage and grid current, as well as their Fast Fourier Transform (FFT) during steady state operation for different current asymmetry. Some differences between the simulation and the experiment can be noticed.

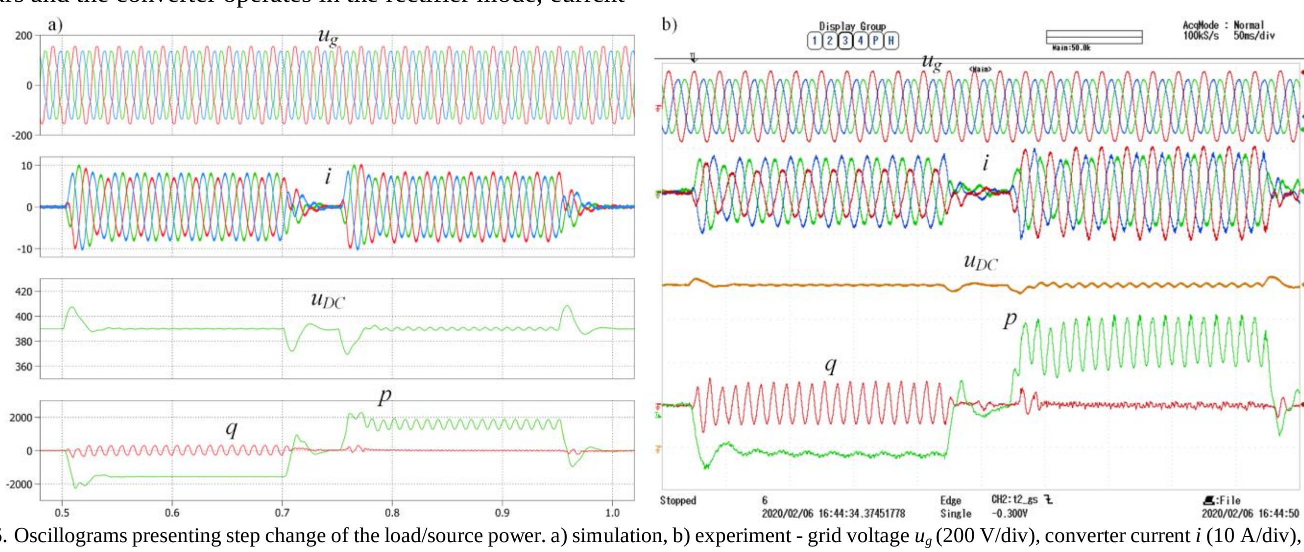

Fig. 6. Oscillograms presenting step change of the load/source power. a) simulation, b) experiment - grid voltage u_g (200 V/div), converter current i (10 A/div), DC link voltage u_{DC} (100 V/div), instantaneous power components p, q (1.2 kW/div).

0093-9994 (c) 2020 IEEE. Personal use is permitted, but republication/redistribution requires IEEE permission. See http://www.ieee.org/publications_standards/publications/rights/index.html for more information.
Authorized licensed use limited to: POLITECHNIKI WARSZAWSKIEJ. Downloaded on July 15,2020 at 23:38:25 UTC from IEEE Xplore. Restrictions apply.

This article has been accepted for publication in a future issue of this journal, but has not been fully edited. Content may change prior to final publication. Citation information: DOI 10.1109/TIA.2020.3009311, IEEE Transactions on Industry Applications

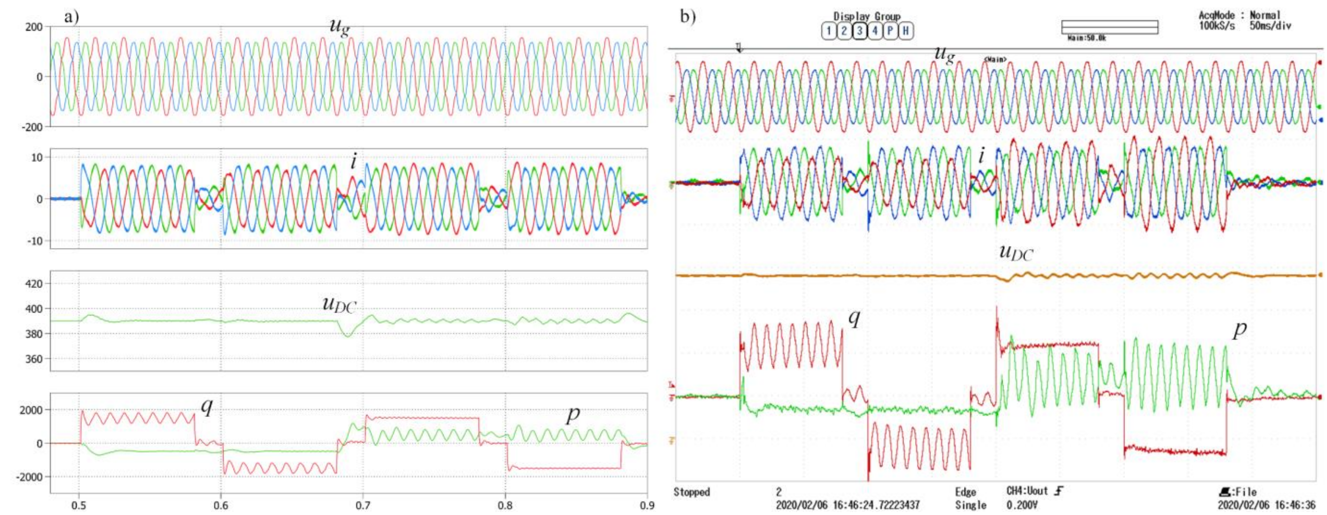

Fig. 7. Oscillograms presenting step change of the reference average q component. a) simulation, b) experiment - grid voltage u_g (200 V/div), converter current i (10 A/div), DC link voltage u_{DC} (100 V/div), instantaneous power components p, q (1.2 kW/div).

Simulated grid voltage is strongly distorted by the 5th and 7th harmonics giving about 9 % of total harmonic distortion (THD). Laboratory grid voltage THD was about 1.5 %. Phase A is marked with the green colour in the simulation whereas in experimental oscillograms it is marked with the red colour. Then dips were induced in different phases, which leads to different hodographs location for the simulation and the experiment. Experimental voltage dip was higher (40 V) than simulated voltage dip (20 V). Although simulated voltage is strongly distorted by high harmonics, their contribution in the current is negligible (THD about 2 %), which confirms low impact of the harmonics on the control system. Experimental current is more distorted (THD about 5%), which is caused by the relatively high dead-time (2.5 μs) applied in the laboratory converter. Simulated current limitation has been achieved properly, while the experimental current waveform slightly exceeds 10 A, due to imperfection of current sensing probes, which also causes different current amplitudes in phases, with the same grid voltage fundamental harmonic amplitudes.

IV. Conclusion

The paper presents an instantaneous power components novel control method of the grid-connected three-phase power converter which operates under grid voltage asymmetry and harmonics. The contribution of proposed method is that the converter current can be asymmetrical, so can provide negative sequence current component through determination of desired power components oscillations depending on their average values and voltage asymmetry level. Derived oscillating reference signals of instantaneous power components keeps limitation of the unbalanced phase current not to exceed maximum current value in any phase. The method does not require symmetrical sequences decomposition and trigonometric transformations since instantaneous power components are independent on frame selection. Moreover, a current balancing method, providing limitation of the three-phase current amplitudes, has been proposed. It provides that when the priority is on active power delivery, the current

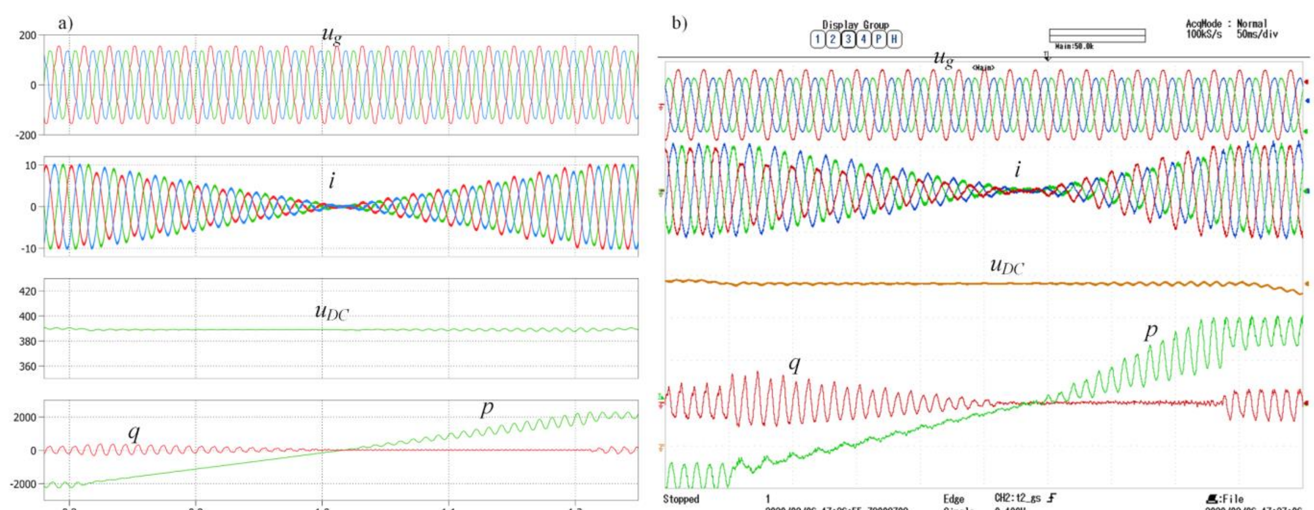

Fig. 8. Oscillograms presenting linear change of load/source power. a) simulation, b) experiment - grid voltage u_g (200 V/div), converter current i (10 A/div), DC link voltage u_{DC} (100 V/div), instantaneous power components p, q (1.2 kW/div).

0093-9994 (c) 2020 IEEE. Personal use is permitted, but republication/redistribution requires IEEE permission. See http://www.ieee.org/publications_standards/publications/rights/index.html for more information.
Authorized licensed use limited to: POLITECHNIKI WARSZAWSKIEJ. Downloaded on July 15,2020 at 23:38:25 UTC from IEEE Xplore. Restrictions apply.

This article has been accepted for publication in a future issue of this journal, but has not been fully edited. Content may change prior to final publication. Citation information: DOI 10.1109/TIA.2020.3009311, IEEE Transactions on Industry Applications

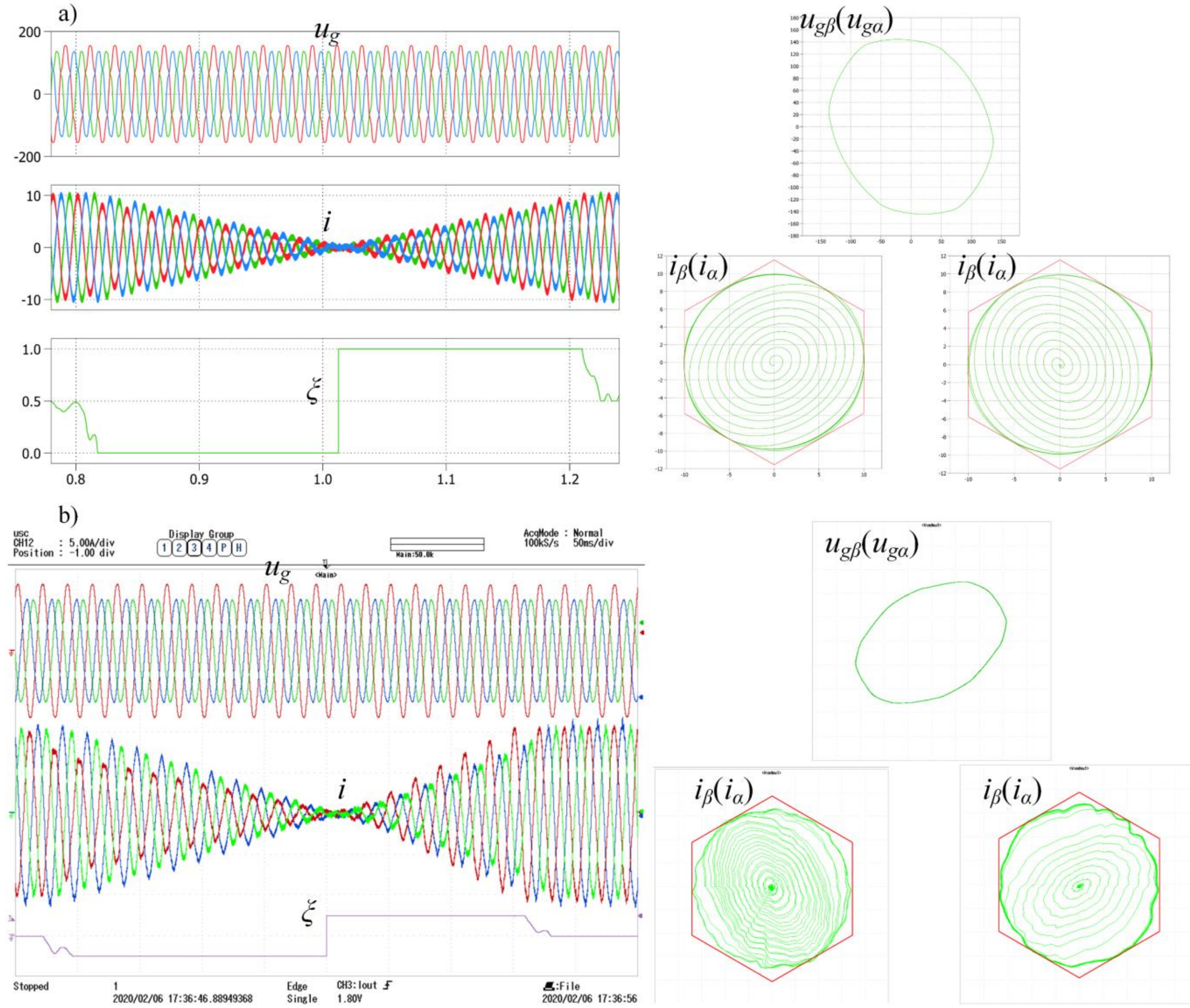

Fig. 9. Oscillograms presenting current balancing during linear change of load/source power and hodographs representing grid voltage and current vector. The left current hodograph corresponds to the left side of the oscillogram and the right hodograph corresponds to the right side of the oscillogram. a) simulation, b) experiment - grid voltage u_g (100 V/div), converter current i (5 A/div), ξ (1/div).

asymmetry decreases to increase average value of instantaneous p power component (which is definitional active power). In general, proposed current balancing method allows for increase converter apparent power. Results of the simulation and experimental tests confirm the assumptions. The system features good dynamic of p and q control, as well as sinusoidal steady-state current.

ACKNOWLEDGMENT

The Work is supported by the National Science Centre (Poland) within the Project granted on the basis of decision number 2016/23/B/ST7/03942.

0093-9994 (c) 2020 IEEE. Personal use is permitted, but republication/redistribution requires IEEE permission. See http://www.ieee.org/publications_standards/publications/rights/index.html for more information.
Authorized licensed use limited to: POLITECHNIKI WARSZAWSKIEJ. Downloaded on July 15,2020 at 23:38:25 UTC from IEEE Xplore. Restrictions apply.

This article has been accepted for publication in a future issue of this journal, but has not been fully edited. Content may change prior to final publication. Citation information: DOI 10.1109/TIA.2020.3009311, IEEE Transactions on Industry Applications

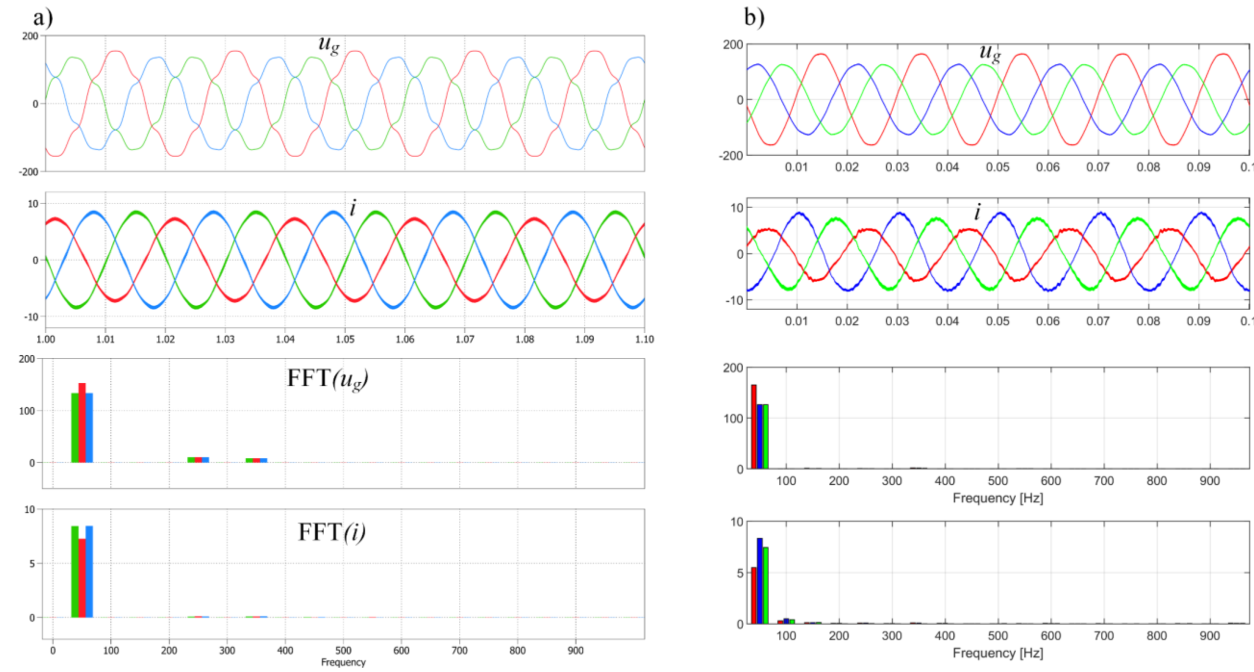

Fig. 10. Oscillograms presenting grid voltage u_g and converter current i and their FFT for current asymmetry opposite to voltage asymmetry. a) simulation, b) experiment.

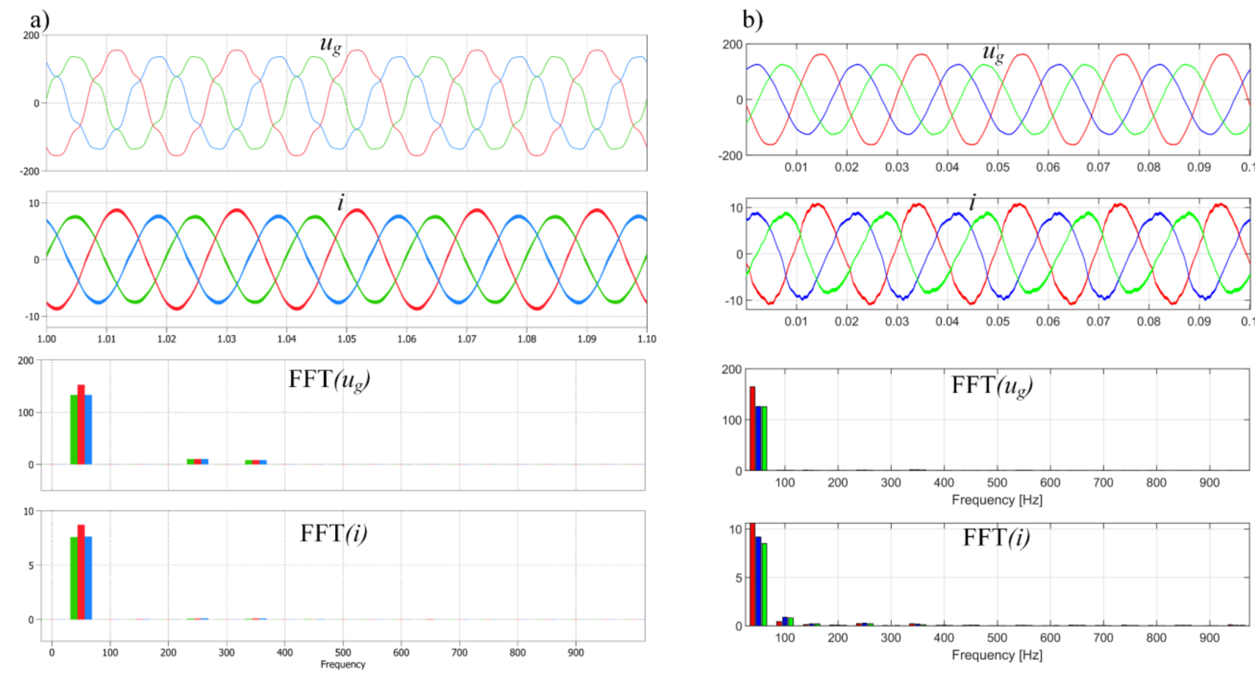

Fig. 11. Oscillograms presenting grid voltage u_g and converter current i and their FFT for current asymmetry corresponding to voltage asymmetry. a) simulation, b) experiment.

0093-9994 (c) 2020 IEEE. Personal use is permitted, but republication/redistribution requires IEEE permission. See http://www.ieee.org/publications_standards/publications/rights/index.html for more information.
Authorized licensed use limited to: POLITECHNIKI WARSZAWSKIEJ. Downloaded on July 15,2020 at 23:38:25 UTC from IEEE Xplore. Restrictions apply.

This article has been accepted for publication in a future issue of this journal, but has not been fully edited. Content may change prior to final publication. Citation information: DOI 10.1109/TIA.2020.3009311, IEEE Transactions on Industry Applications

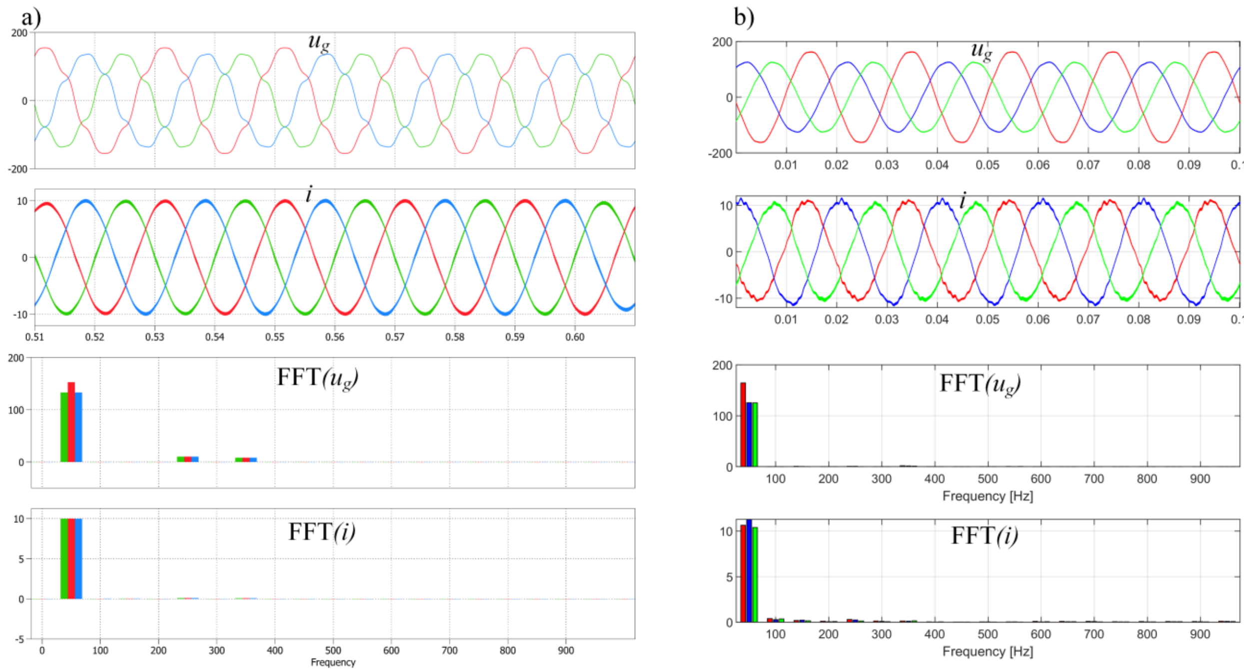

Fig. 12. Oscillograms presenting grid voltage u_g and converter current i and their FFT for current close to symmetrical. a) simulation, b) experiment.

References

[1] S. Wodyk, G. Iwanski, “Control of Three-Phase Power Electronic Converter with Power Controllers in Stationary Frame,” 2019 Fourteenth Int. Conf. Ecological Vehicles and Renewable Energies (EVER), Monte-Carlo, Monaco, 2019

[2] N. R. Zargari and G. Joos, “Performance investigation of a current controlled voltage - regulated PWM rectifier in rotating and stationary frames”, Int. Conf. Ind. Electron. Control Instrum., Maui, HI, USA, 1993, pp. 1193–119.

[3] C. T. Rim et al., “A complete DC and AC analysis of three-phase controlled-current PWM rectifier using circuit D-Q transformation”, IEEE Trans. Power Electron., vol. 9, no. 4, pp. 390–396, Jul. 1994.

[4] T. Ohnishi, “Three-phase PWM converter/inverter by means of instantaneous active and reactive power control”, Ind. Electron. Conf. - ECON’91, Kobe, Japan, 1991, pp. 819-824.

[5] S. K. Chung, “Phase-locked loop for grid-connected three-phase power conversion systems”, IEE Proc. – Elect. Pow. Appl., vol. 147, no. 3, pp. 213-219, May 2000.

[6] J. L. Duarte, A. Van Zwam, C. Wijnands, A. Vandenput, “Reference frames fit for controlling PWM rectifiers”, IEEE Trans. Ind. Electron., Vol. 46, No. 3, pp. 628-630, June 1999.

[7] M. Malinowski, M. P. Kazmierkowski, S. Hansen, F. Blaabjerg, G. D. Marques, “Virtual flux based Direct Power Control of three-phase PWM rectifier”, IEEE Trans. Ind. Appl., vol. 37, no. 4, pp. 1019-1027, Jul/Aug 2001.

[8] M. Malinowski, M. Jasiński, and M. P. Kazmierkowski, “Simple Direct Power Control of Three-Phase PWM Rectifier Using Space-Vector Modulation (DPC-SVM)”, IEEE Trans. Ind. Electron, vol. 51, no. 2, pp. 447– 454, April 2004.

[9] Y. Sato, T. Ishizuka, K. Nezu, T. Kataoka, “A new control strategy for voltage-type PWM rectifiers to realize zero steady-state control error in input current”, IEEE Trans. Ind. Appl., Vol. 34, No. 3, pp. 480-486, May-June 1998

[10] D. N. Zmood, D. G. Holmes, “Stationary frame current regulation of PWM inverters with zero steady-state error”, IEEE Trans. Power Electron., Vol. 18, No. 3, pp. 814-822, May 2003.

[11] J. G. Hwang, M. Winkelnkemper, P. W. Lehn, “Design of an Optimal Stationary Frame Controller for Grid Connected AC-DC Converters”, IECON 2006 - 32nd Annual Conf. on IEEE Ind. Electron., Paris, 2006, pp. 167-172.

[12] D. G. Holmes, T. A. Lipo, B. P. McGrath, W. Y. Kong, “Optimized Design of Stationary Frame Three Phase AC Current Regulators”, IEEE Trans. Power Electron., Vol. 24, No. 11, pp. 2417-2426, Nov. 2009.

[13] J. G. Hwang, P. W. Lehn, M. Winkelnkemper, “A Generalized Class of Stationary Frame-Current Controllers for Grid-Connected AC–DC Converters”, IEEE Trans. Power Delivery, Vol. 25, No. 4, pp. 2742-2751, Oct. 2010.

[14] C. Zou, B. Liu, S. Duan, R. Li, “Stationary Frame Equivalent Model of Proportional-Integral Controller in dq Synchronous Frame”, IEEE Trans. Power Electron., Vol. 29, No. 9, pp. 4461-4465, Sept. 2014.

[15] D. Roiu, R. I. Bojoi, L. R. Limongi, A. Tenconi, “New Stationary Frame Control Scheme for Three-Phase PWM Rectifiers under Unbalanced Voltage Dips Conditions”, IEEE Trans. Ind. Appl., vol. 46, no. 1, pp. 268-277, Jan.-Feb. 2010.

[16] Z. Li, Y. Li, P. Wang, H. Zhu, C. Liu and W. Xu, “Control of Three-Phase Boost-Type PWM Rectifier in Stationary Frame under Unbalanced Input Voltage,” IEEE Trans. Power Electron., vol. 25, no. 10, pp. 2521-2530, Oct. 2010.

[17] F. Wang, J. L. Duarte and M. A. M. Hendrix, “Pliant Active and Reactive Power Control for Grid-Interactive Converters under Unbalanced Voltage Dips,” IEEE Trans. Power Electron., vol. 26, no 5, May 2011.

[18] A. Camacho, M. Castilla, J. Miret, A. Borrell and L. G. de Vicuña, “Active and Reactive Power Strategies with Peak Current Limitation for Distributed Generation Inverters during Unbalanced Grid Faults,” IEEE Trans. on Ind. Electron., vol. 62, no. 3, pp. 1515-1525, March 2015.

[19] G. Iwanski, T. Luszczyk and M. Szypulski, “Virtual-Torque-Based Control of Three-Phase Rectifier under Grid Imbalance and Harmonics”, IEEE Trans. Power Electron., vol. 32, no. 9, pp. 6836-6852, Sept. 2017.

[20] G. Iwanski, “Virtual Torque and Power Control of a Three-Phase Converter Connected to an Unbalanced Grid with Consideration of Converter Current Constraint and Operation Mode,” IEEE Trans. Power Electron., vol. 34, no. 4, pp. 3804-3818, April 2019.

[21] P. Rioual, H. Pouliquen and J.-P. Louis,” Regulation of a PWM rectifier in the unbalanced network state using a generalized model,” IEEE Trans. Power Electron., vol. 11, no. 3, pp. 495-502, May 1996.

[22] A. G. Yepes, A. Vidal, O. López and J. Doval-Gandoy, "Evaluation of Techniques for Cross-Coupling Decoupling Between Orthogonal Axes in Double Synchronous Reference Frame Current Control," IEEE Trans. on Ind. Electron., vol. 61, no. 7, pp. 3527-3531, July 2014.

[23] M. Malinowski, G. Marques, M. Cichowlas and M. P. Kazmierkowski, “New direct power control of three-phase PWM boost rectifiers under distorted and imbalanced line voltage conditions,” 2003 IEEE Int. Symp. Ind. Electron., Rio de Janeiro, Brazil, 2003, pp. 438-443 vol. 1.

[24] Y. Gui, C. Kim, C. C. Chung, J. M. Guerrero, Y. Guan and J. C. Vasquez, “Improved Direct Power Control for Grid-Connected Voltage Source Converters,” IEEE Trans. Ind. Electron., vol. 65, no. 10, pp. 8041-8051, Oct. 2018,

0093-9994 (c) 2020 IEEE. Personal use is permitted, but republication/redistribution requires IEEE permission. See http://www.ieee.org/publications_standards/publications/rights/index.html for more information.
Authorized licensed use limited to: POLITECHNIKI WARSZAWSKIEJ. Downloaded on July 15,2020 at 23:38:25 UTC from IEEE Xplore. Restrictions apply.

This article has been accepted for publication in a future issue of this journal, but has not been fully edited. Content may change prior to final publication. Citation information: DOI 10.1109/TIA.2020.3009311, IEEE Transactions on Industry Applications

[25] H. Nian, Y. Shen, H. Yang and Y. Quan, "Flexible Grid Connection Technique of Voltage-Source Inverter under Unbalanced Grid Conditions Based on Direct Power Control," IEEE Trans. Ind. Appl., vol. 51, no. 5, pp. 4041-4050, Sept.-Oct. 2015.

[26] Y. Zhang and C. Qu, "Direct Power Control of a Pulse Width Modulation Rectifier Using Space Vector Modulation under Unbalanced Grid Voltages," IEEE Trans. Power Electron., vol. 30, no. 10, pp. 5892-5901, Oct. 2015.

[27] Y. Zhang, J. Liu, H. Yang and J. Gao, "Direct Power Control of Pulse Width Modulated Rectifiers without DC Voltage Oscillations under Unbalanced Grid Conditions," IEEE Trans. Ind. Electron., vol. 65, no. 10, pp. 7900-7910, Oct. 2018.

[28] W. Jiang, Y. Wang, J. Wang, L. Wang and H. Huang, "Maximizing Instantaneous Active Power Capability for PWM Rectifier Under Unbalanced Grid Voltage Dips Considering the Limitation of Phase Current," in IEEE Trans. Ind. Electron., vol. 63, no. 10, pp. 5998-6009, Oct. 2016.

[29] Z. Xin, X. Wang, Z. Qin, M. Lu, P. C. Loh and F. Blaabjerg, "An Improved Second-Order Generalized Integrator Based Quadrature Signal Generator,", IEEE Trans. Power Electron., vol. 31, no. 12, pp. 8068-8073, Dec. 2016.

0093-9994 (c) 2020 IEEE. Personal use is permitted, but republication/redistribution requires IEEE permission. See http://www.ieee.org/publications_standards/publications/rights/index.html for more information.
Authorized licensed use limited to: POLITECHNIKI WARSZAWSKIEJ. Downloaded on July 15,2020 at 23:38:25 UTC from IEEE Xplore. Restrictions apply.